# Educational Software Bundle for Studying Magnetotelluric Theory and Specific Geoelectric Structure Models

DESPINA KALISPERI[2], GEORGE HLOUPIS[2], JOHN P. MAKRIS[1], DEREK RUST[3], FILIPPOS VALLIANATOS[2], VASSILIOS SALTAS[2], PANTELIS SOUPIOS[2], and IOANNIS O. VARDIAMBASIS[1]

1)  Department of Electronics
Technological Educational Institute of Crete
3, Romanou St, Chania, Crete Island
GREECE

2)  Department of Natural Resources & Environment
Technological Educational Institute of Crete
3, Romanou St, Chania, Crete Island
GREECE

3)  Department of Geography and Earth Sciences,
Brunel University
Uxbridge, Middlesex, UB8 3PH, England
UNITED KINGDOM
http://www.chania.teicrete.gr

*Abstract:*- Magnetotellurics is of one the most important and extensively applied research and exploration methodologies in electromagnetic geophysics engineering. On the other hand, many educational difficulties are reported concerning the level of comprehension and the depth of understanding of the learners with respect to magnetotellurics, as well as the development, by the tutors, of educational tools and methods for effective teaching of the various aspects of magnetotelluric theory. Aiming to contribute to improve these conditions, an educational software bundle was developed in order to provide configurable modelling and simulation tools of impedance tensor decomposition, distortion tensor decomposition, and Mohr circle topology in the context of different, user-definable geoelectric structure symmetries. Indicative examples are presented that demonstrate the mode of application of the various software modules in studying interesting magnetotelluric theoretical aspects and problems.

*Key-Words*: - Education, magnetotelluric, geoelectric structure, impedance tensor, decomposition, Mohr circle

## 1  Introduction

The magnetotelluric (MT) method is an efficient technique for mapping the subsurface electrical conductivity structure. The method assumes a linear relationship between the horizontal natural magnetic and electric fields at the earth's surface, over a broad frequency range and independent of source polarization and position. The field transfer function, termed the impedance tensor, is estimated in the frequency domain from the experimental MT-data.

The extraction from the data of scalar parameters that will have interpretable physical meaning in terms of the actual conductivity structure within the earth is the aim of the impedance tensor analysis.

The MT-study proceeds in two consecutive stages; the first is the conventional MT-analysis where the electromagnetic response of the subsurface hemispace is considered as unified, while in the subsequent, the impedance tensor is decomposed in more than one tensors.

The magnetotelluric theory is, conceptually, the application of the electromagnetic theory and the electromagnetic wave propagation theory in the case of the solid Earth. This nature makes magnetotellurics a very challenging yet exacting engineering education field. Contextually, difficulties are expected to exist referring to comprehension level and depth of understanding of the learners as well as to the tutoring tools and methods, developed to teach efficiently the various aspects of magnetotelluric theory.

The present work outlines a Magnetotelluric Educational Software Bundle, hereafter abbreviated as MT-ESB, developed to provide configurable model-

ling and simulation tools of impedance tensor decomposition, distortion tensor decomposition, and Mohr circle topology in the context of different, user-definable geoelectric structure symmetries. The mode of application of MT-ESB consisting modules is demonstrated by their implementation to specific, indicative yet educationally interesting MT-theoretical problems.

The MT-ESB development was based on Excel 2003[TM] platform [17]. Excel 2003[TM] spreadsheet software module is part of the Microsoft Office 2003[TM] suite. It enables the user to turn different kinds of data into information with powerful tools for data processing and analysis as well as results communicating and sharing. Excel 2003[TM] was selected because it builds on its commitment to reliable and accurate numerical analysis and due to its broad recognition and use.

## 2  MT-ESB and Tensor Decomposition

### 2.1 MT-ESB in studying distortion tensor decomposition

It is considered that the Earth consists of a 1D or 2D-basement termed as *regional structure* (i.e., the horizontal dimensions of which are comparable with the penetration depth) coupled with local (compared to the penetration depth) 3D-zones of anomalous conductivity. These near surface anomalies act as *semi-static scatterers* (usually called *galvanic*) that mainly affect the observed electric field in direction and magnitude [3], [4].

Physically, 3D-galvanic distortion is caused by the presence of electric charges at discontinuities or gradients in electrical conductivity. The local 3D-surface structure causes the observed magnetotelluric impedance tensor to be a location dependent mixture of the local and regional responses; this can include distortion of both in magnitude and phase. In such cases, Groom and Bailey [3], [4], [5] suggested a decomposition of the measured impedance tensor:

$$\vec{Z}_m = \hat{R}g\vec{T}\vec{S}\vec{A}\vec{Z}_{2D}\hat{R}^t = \hat{R}\vec{T}\vec{S}\vec{Z}'_{2D}\hat{R}^t \quad (1)$$

with:

$$\vec{C} = g\vec{T}\vec{S}\vec{A} = g\begin{pmatrix} 1 & -t \\ t & 1 \end{pmatrix}\begin{pmatrix} 1 & e \\ e & 1 \end{pmatrix}\begin{pmatrix} 1+s & 0 \\ 0 & 1-s \end{pmatrix} \quad (2)$$

and:

$$\vec{Z}'_{2D} = g\begin{pmatrix} 0 & (1+s)Z^E \\ -(1-s)Z^H & 0 \end{pmatrix} = \begin{pmatrix} 0 & \alpha' \\ -b' & 0 \end{pmatrix} \quad (3)$$

where $\hat{R}$ is the operator of clockwise rotation at an angle $\vartheta$ of the measuring system, in order to coincide with the principal axes of the 2D-structure:

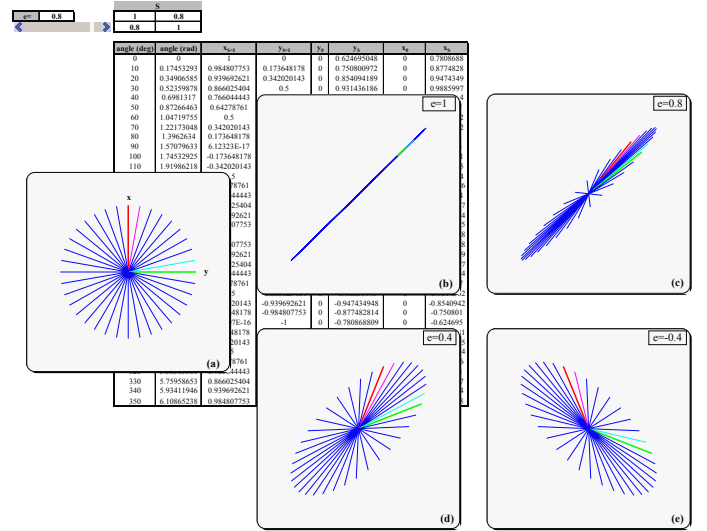$$\hat{R} = \begin{pmatrix} \cos\vartheta & \sin\vartheta \\ -\sin\vartheta & \cos\vartheta \end{pmatrix} \quad (4)$$



**Fig.1.** A family of unit vectors **(a)** before and **(b), (c), (d), (e)** after the application of the shear distortion tensor.

$\vec{C}$ is the distortion tensor, g is the gain of the measuring site, $\vec{T}$ is the twist tensor, $\vec{S}$ is the shear tensor, $\vec{A}$ is the local anisotropy tensor and $\vec{Z}'_{2D}$ is the tensor that refers to an ideal 2D-regional structure at its principal coordinate system, but includes also $g\vec{A}$, which does not destroy its ideal form. It must be clarified that this is adopted because the local anisotropy (with intrinsic system that is identical with the principal axis system of the regional structure) cannot be distinguished experimentally from the regional anisotropy except for cases where the latter is known independently.

A physical insight into the effect of each one of these distortion tensors on the regional electric field can be obtained by studying the effects of the tensors $\vec{T}$, $\vec{S}$ and $\vec{A}$, on a family of unit vectors by using accordingly the relative module of the developed MT-ESB.

As an example, the shear tensor, $\vec{S}$, generates an anisotropy in directions which bisect the regional principal axes. In the graphs produced by MT-ESB (see Fig.1) it is depicted that the vectors that are aligned with the regional principal directions exhibit the greater angular deviations (e.g. a vector on the x-axis is rotated clockwise by an angle $\varphi_e = \tan^{-1} e$, and a vector on the y-axis is rotated counter-clockwise by the same angle). A physical explanation of such type of distortion may be the concentration of current into a long conductive channel.
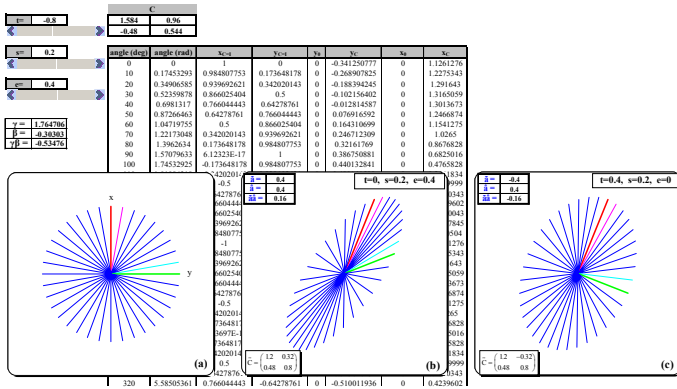
| t= | -0.8 | | C | |
|---|---|---|---|---|
| | | | 1.584 | 0.96 |
| s= | 0.2 | | -0.48 | 0.544 |
| e= | 0.4 | | | |
| γ = | 1.764706 | | | |
| β = | -0.30303 | | | |
| γβ = | -0.53476 | | | |

| angle (deg) | angle (rad) | xc-a | yc-a | ya | yc | xb | xc |
|---|---|---|---|---|---|---|---|
| 0 | 0 | 1 | 0 | 0 | -0.341250777 | 0 | 1.1261276 |
| 10 | 0.17453293 | 0.984807753 | 0.173648178 | 0 | -0.268907825 | 0 | 1.2275343 |
| 20 | 0.34906585 | 0.939692621 | 0.342020143 | 0 | -0.188394245 | 0 | 1.291643 |
| 30 | 0.52359878 | 0.866025404 | 0.5 | 0 | -0.102156402 | 0 | 1.3165059 |
| 40 | 0.6981317 | 0.766044443 | 0.64278761 | 0 | -0.012814587 | 0 | 1.3013673 |
| 50 | 0.87266463 | 0.64278761 | 0.766044443 | 0 | 0.076916592 | 0 | 1.2466874 |
| 60 | 1.04719755 | 0.5 | 0.866025404 | 0 | 0.164310699 | 0 | 1.1541275 |
| 70 | 1.22173048 | 0.342020143 | 0.939692621 | 0 | 0.246712309 | 0 | 1.0265 |
| 80 | 1.3962634 | 0.173648178 | 0.984807753 | 0 | 0.32161769 | 0 | 0.8676828 |
| 90 | 1.57079633 | 6.12323E-17 | 1 | 0 | 0.386150881 | 0 | 0.6825016 |
| 100 | 1.74532925 | -0.173648178 | 0.984807753 | 0 | 0.440132841 | 0 | 0.4765828 |
| 320 | 5.58505361 | 0.766044443 | -0.64278761 | 0 | -0.510011936 | 0 | 0.4239602 |

Fig.2 graphs:
- (a)
- t=0, s=0.2, e=0.4; $\bar{a}$ = 0.4, $\bar{a}$ = 0.4, $\bar{a}$ = 0.16 (b); $C = \begin{pmatrix} 1.2 & 0 \\ 0.48 & 0.8 \end{pmatrix}$
- t=0.4, s=0.2, e=0 (c); $\bar{a}$ = -0.4, $\bar{a}$ = 0.4, $\bar{a}$ = -0.16; $C = \begin{pmatrix} 1.2 & -0.32 \\ 0.48 & 0.8 \end{pmatrix}$

**Fig.2** A family of unit vectors before **(a)** and after: **(b)** the application of a distortion tensor with shear and anisotropy, **(c)** the application of a distortion tensor with twist and anisotropy.

## 2.1.1 MT-ESB in examining the uniqueness of the distortion tensor decomposition

The distortion tensor, $\ddot{C}$, is written analytically:

$$\ddot{C} = \frac{g}{\sqrt{\left(1+e^2\right)\left(1+t^2\right)\left(1+s^2\right)}} \begin{pmatrix} (1+s)(1-te) & (1-s)(e-t) \\ (1+s)(e+t) & (1-s)(1+te) \end{pmatrix} \quad (5)$$

If weak distortions are considered (i.e., t, e and s much smaller than unity), 2nd-order terms can be ignored for the parameters e, s and t, and then eq. (5) becomes:

$$\ddot{C} = \begin{pmatrix} C_1 & C_2 \\ C_3 & C_4 \end{pmatrix} \approx g \begin{pmatrix} 1+s & e-t \\ e+t & 1-s \end{pmatrix} \quad (6)$$

Then, the distortion parameters are easily derived from eq. (6):

$$g \approx \frac{C_1+C_4}{2}, \ e \approx \frac{C_2+C_3}{C_1+C_4}, \ s \approx \frac{C_1-C_4}{C_1+C_4}, \ t \approx \frac{C_3-C_2}{C_1+C_4}$$

In eq. (5) the normalizing factors are actually incorporated into g. Groom and Bailey [4] defined:

$$\gamma = \frac{C_2}{C_4} = \frac{e-t}{1+te}, \quad \text{if} \ C_4 \neq 0 \quad (7)$$

$$\beta = \frac{C_3}{C_1} = \frac{e+t}{1-te}, \quad \text{if} \ C_1 \neq 0 \quad (8)$$

In order to understand the meaning of these parameters, the MT-ESB can be implemented in the theoretical examination of the following special cases:

♦ If $\gamma = \beta$ there is a unique solution:

$$t = 0, \ e = \gamma = \beta, \ g = \frac{C_1+C_4}{2}, \ s = \frac{C_1-C_4}{2g}$$

♦ If $\gamma = -\beta$, then there is also a unique solution:

$$e = 0, \ t = -\gamma = \beta, \ g = \frac{C_1+C_4}{2}, \ s = \frac{C_1-C_4}{2g}$$

The MT-ESB's graphs depict the effects at the family of the unity vectors of the distortion tensors which satisfy the restrictions $\gamma = \beta$ or $\gamma = -\beta$ (see Fig.2).

## 2.1.2 MT-ESB simulates geoelectric structure's distorting effect on electrotelluric field

It is usually assumed [3] that the earth is essentially flat with a 2D-conductivity structure on a broad regional scale; this assumption implies that any 3D-structures are all inductively weak. In the principal axis system of this 2D-structure (i.e. x-horizontal axis is along the strike of the structure and the vertical axis is normal to the earth's surface), the *regional* horizontal electric field components, $\bar{e}_r$, and magnetic field components, $\bar{h}_r$, are linearly related:

$$\bar{e}_r = \begin{pmatrix} 0 & \alpha \\ -b & 0 \end{pmatrix} \bar{h}_r = \ddot{Z}_{2D} \bar{h}_r \quad (9)$$

where α denotes the quantity $Z_\perp$ which is the impedance associated with the 2D-mode containing current only perpendicular to the strike and b denotes the quantity $Z_\parallel$, the impedance associated with the mode containing current only parallel to the strike. When the horizontal electric field $\bar{e}$ and the horizontal magnetic field $\bar{h}$ are measured at a point of the earth surface, they deviate from the regional values $\bar{e}_r$ and $\bar{h}_r$, due to the local conductivity variations. The electric field can be strongly distorted by charges that are accumulated on conductivity gradients or boundaries; on the other hand, the magnetic field is not so strongly disturbed since it is due to a weighted spatial average of the telluric current density over a much larger volume. Therefore, we are justified to adopt the approximation: $\bar{h} \cong \bar{h}_r$, but the electric field $\bar{e}$ should be related to $\bar{e}_r$ through a distortion or channelling tensor, $\ddot{C}$ [1], [2]:

$$\bar{e} = \ddot{C} \cdot \bar{e}_r = \begin{pmatrix} C_1 & C_2 \\ C_3 & C_4 \end{pmatrix} \bar{e}_r \quad (10)$$

In the presence of small-scale surface scatterers (which are assumed to be inductively weak), their effects can be considered as frequency independent and the elements of the tensor $\ddot{C}$ as real numbers. In absence of distortions, $\ddot{C}$ will reduce to the identity tensor, $\ddot{I}$.

In the case of a galvanic distortion and in order to recover information concerning the two-dimensional impedances, it has been shown ([1], [18]) that the exact knowledge of the elements of $\ddot{C}$ is not necessary. The decomposition of the measured impedance tensor, however, it is a requisite to be done uniquely.
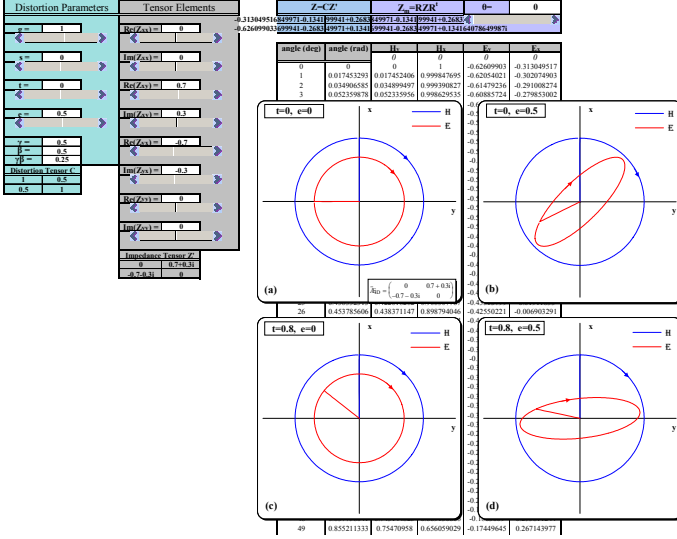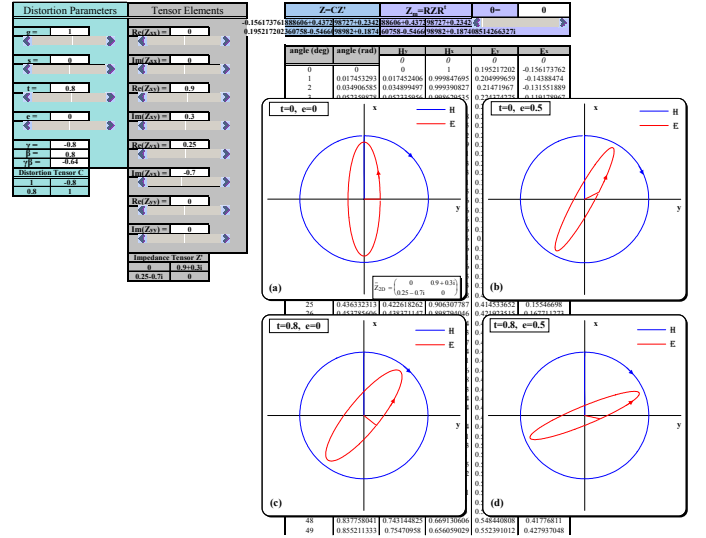
**Fig.3** The geometrical locus of the electric field vector trace as a result of the rotation of the incident horizontal linearly polarised unitary magnetic field, **(a)** for an ideal 1D-structure; **(b)**, **(c)**, **(d)** for a 1D-regional structure, but with the presence of a near surface semi-static scatterer, with different distortion parameters.

In the intrinsic (or principal axes) system of the regional structure, the impedance tensor that refers to the 2D-structure obeys the relation:

$$\vec{e}_r = \vec{\vec{Z}}_{2D}\vec{h}_r$$

which, using eq. (10), gives:

$$\vec{e} = \vec{\vec{C}}\vec{\vec{Z}}_{2D}\vec{h}_r \tag{11}$$

or in the measuring coordinate system:

$$\vec{e} = \hat{R}\vec{\vec{C}}\vec{\vec{Z}}_{2D}\hat{R}^t\vec{h} = \vec{\vec{Z}}_m\vec{h} \tag{12}$$

where $\vec{\vec{Z}}_m$ is the measured impedance tensor, $\vec{\vec{Z}}_{2D}$ is the regional 2D-tensor in the regional inductive principal axis system [i.e., it has the form of eq. (9)], $\vec{\vec{C}}$ is the distortion tensor expressed also at the regional intrinsic system and $\hat{R}$ is the rotation operator which performs the transformation of vectors from the principal axis system to the measurement axis system.

Based on context presented in this sub-section, a suitably customized module of MT-ESB has been developed, in order to simulate the distorting effect of a semi-static scatterer on the regionally induced electric field for different orders of symmetry of the regional geoelectric structure and for different types of scatterers. This is demonstrated indicatively in Fig.3 and Fig.4 for the cases of 1D and 2D geoelectric structure symmetries respectively.

## 2.2 MT-ESB in studying MT-tensor decomposition set of parameters

This decomposition is described through seven real parameters:

♦ the scaled real and imaginary parts of the major principal impedance $\alpha'$ (or equivalently the major apparent resistivity and phase),

♦ the scaled real and imaginary parts of the minor principal impedance $b'$ (or equivalently the minor apparent resistivity and phase),

♦ the azimuth angular deviation $\vartheta$ between the principal axis system of the regional structure and the measuring coordinate system,

♦ the shear parameter e and

♦ the twist parameter t.



**Fig.4** The geometrical locus of the electric field vector trace as a result of the rotation of the incident, horizontal linearly polarised unitary magnetic field, **(a)** for an ideal 2D-structure; **(b)**, **(c)**, **(d)** for a 2D-regional structure, but with the presence of a near surface semi-static scatterer, with different distortion parameters.

In order to determine the above parameters and based on a modified form of the Pauli spin matrices [15]:

$$\vec{\vec{I}} = \begin{pmatrix} 1 & 0 \\ 0 & 1 \end{pmatrix}, \quad \vec{\vec{\Sigma}}_1 = \begin{pmatrix} 0 & 1 \\ 1 & 0 \end{pmatrix}, \quad \vec{\vec{\Sigma}}_2 = \begin{pmatrix} 0 & -1 \\ 1 & 0 \end{pmatrix}, \quad \vec{\vec{\Sigma}}_3 = \begin{pmatrix} 1 & 0 \\ 0 & -1 \end{pmatrix}$$

a useful factorization of the measured impedance is achieved:

$$\vec{\vec{Z}}_m = \frac{1}{2}\left(\alpha_0^m\vec{\vec{I}} + \alpha_1^m\vec{\vec{\Sigma}}_1 + \alpha_2^m\vec{\vec{\Sigma}}_2 + \alpha_3^m\vec{\vec{\Sigma}}_3\right) \tag{13}$$

where:

$$\alpha_0^m = Z_{xx} + Z_{yy} \tag{14}$$

$$\alpha_1^m = Z_{xy} + Z_{yx} \tag{15}$$

$$\alpha_2^m = Z_{yx} - Z_{xy} \tag{16}$$

$$\alpha_3^m = Z_{xx} - Z_{yy} \tag{17}$$

By substituting eq. (13) to eq. (1), the following non-linear system of complex equations is obtained for the coefficients $\alpha_i$ :

$$\alpha_0 = t\sigma + e\delta \tag{18}$$

$$\alpha_1 = (\delta - et\sigma)\cos 2\vartheta - (t\delta + e\sigma)\sin 2\vartheta \tag{19}$$

$$\alpha_2 = -\sigma + et\delta \tag{20}$$

$$\alpha_3 = -(t\delta + e\sigma)\cos 2\vartheta - (\delta - et\sigma)\sin 2\vartheta \tag{21}$$

where: $\sigma = \alpha' + b'$ and $\delta = \alpha' - b'$ (22)

The above system can be solved analytically for the set of the model parameters $(\sigma, \delta, e, t, \vartheta)$ from the experimental data, by restricting the azimuth angle to $0 \le \vartheta \le \pi$. Thus, MT-tensor decomposition successfully determines the dimensionality of the dominant geoelectric structure and recovers the regional impedance responses except for the "static-shift" influence [in cases, of course, where the regional structure can be characterized approximately as 1D or 2D, ("superimposition model")].

Moreover, the principal directions of the regional induction are determined but with the ambiguity concerning the strike-direction.

MT-ESB has been designed to provide a practical, graphical tool to investigate the latter solution multiplicity by applying the argument that if $(\sigma, \delta, e, t, \vartheta)$ is a solution-set of the system (18-21), then $\left(-e, t, \sigma, -\delta, \vartheta + \dfrac{\pi}{2}\right)$ is also a solution-set and it is depicted with the example of Fig.5.

## 2.3 MT-ESB's comparison between tensor decomposition and conventional MT-analysis

Let us assume that the measured impedance tensor results from a local galvanic distortion of the regionally induced electric field at a large-scale conductivity structure with at most 2D-symmetry and that the magnetic field distortion is negligible.

One of the most interesting parameters for the modelling of the earth conductivity structure is the azimuth angle $\vartheta$ (*strike*-angle) which denotes the azimuth angular deviation of the regional principal axis system from the measuring coordinate system.

The conventional method [14], [16], determines the strike-angle by minimizing the quantity $\left|Z_{xx}(\vartheta')\right|^2 + \left|Z_{yy}(\vartheta')\right|^2$, or equivalently by minimizing the quantity $\left|\alpha_3(\vartheta')\right|^2$, where:

$$\alpha_3(\vartheta') = -(t\delta + e\sigma)\cos 2(\vartheta - \vartheta') - \\ - (\delta - et\sigma)\sin 2(\vartheta - \vartheta') \tag{23}$$

If the local inhomogeneities influence the induced electric field only with anisotropy distortion (s≠0, t=0, e=0), then eq. (23) becomes:

$$\alpha_3(\vartheta') = -\delta \sin 2(\vartheta - \vartheta')$$

and the intrinsic system of the regional geoelectric structure is correctly determined. In all the other cases, i.e., where twist $(t \ne 0)$ and/or shear $(e \ne 0)$ are present, the conventionally derived angle $\vartheta'$ will be different from the actual strike-angle, $\vartheta$ .
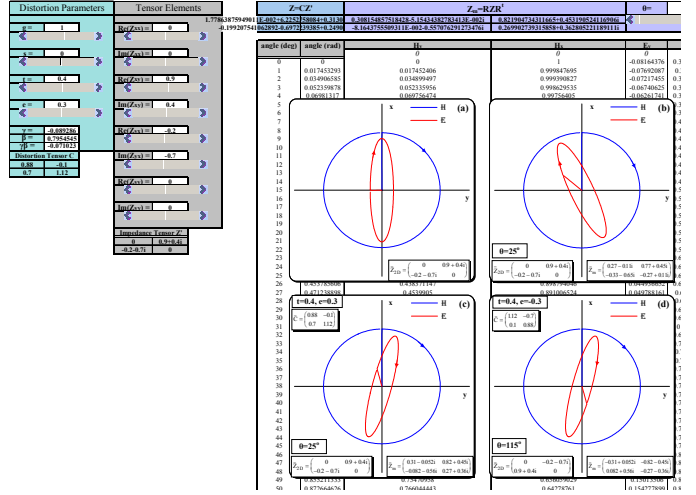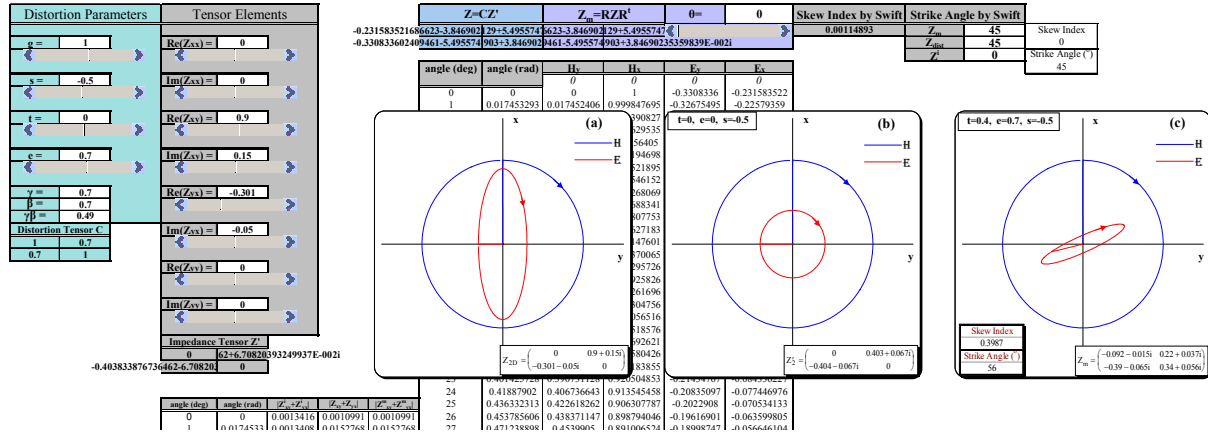


**Fig.5** The geometrical locus of the electric field vector trace as a result of the rotation of the incident horizontal linearly polarised unitary magnetic field, **(a), (b)** for an ideal 2D-structure, when the measuring and the intrinsic co-ordinate systems have an angular deviation of $\vartheta = 0°$ and $\vartheta = 25°$ respectively; **(c), (d)** for a 2D-regional structure for the set of solutions (σ, δ, e, t, $\vartheta$) and (σ, -δ, -e, t, $\vartheta$+90°), but with the presence of a near surface semi-static scatterer, with different distortion parameters respectively.

The latter argument is supported and validated, in a very convenient way, by examining with an MT-ESB's module the following two marginal cases:

*a)* If the tensor $\vec{Z}'_{2D}$ , determined by tensor decomposition, is isotropic, i.e., $\alpha' = b'$ , and thus $\delta \approx 0$ , the conventional analysis gives:

$$\vartheta' = \vartheta - \frac{1}{2}\tan^{-1}\left(\frac{1}{t}\right) = \vartheta \pm \frac{\pi}{4} + \frac{1}{2}\varphi_t \tag{24}$$

with the assumption that $t \ne 0$ (see Fig.6).

*b)* If the tensor $\vec{Z}'_{2D}$ is extremely anisotropic, i.e., $|\alpha'| >> |b'|$ , and thus $\delta \approx \sigma$ , the conventional analysis gives:

$$\vartheta' = \vartheta + \frac{1}{2}\tan^{-1}\left(\frac{t + e}{1 - et}\right) = \vartheta + \frac{1}{2}q \tag{25}$$

with the assumption that both e and t are not zero (see Fig.7).

At the measuring coordinate system (x,y) the MT-data are collected and the impedance tensor, $\vec{Z}_m$, is
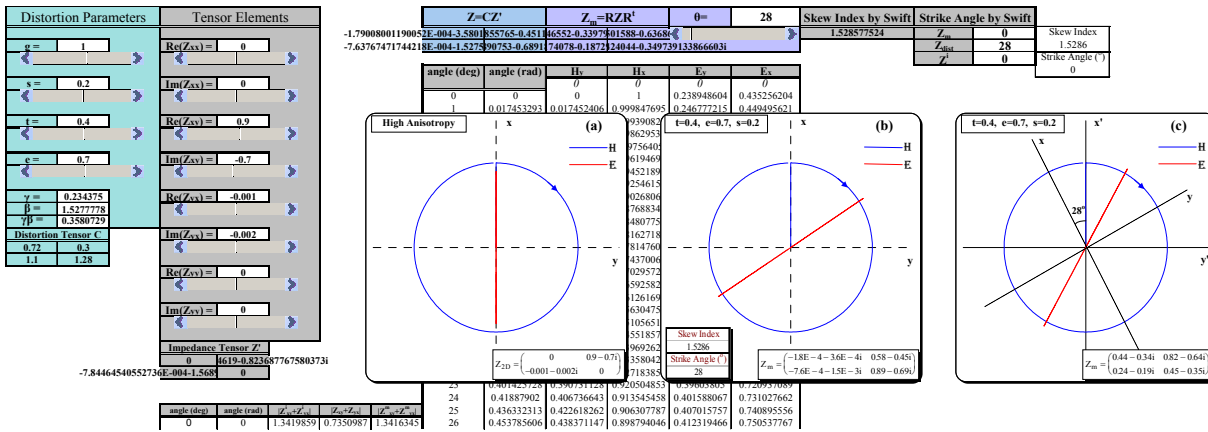


**Fig.6** The geometrical locus of the electric field vector trace as a result of the rotation of the incident horizontal linearly polarised unitary magnetic field, **(a)** for an ideal 2D-structure; **(b)** for a 2D-regional structure, with the presence of a local near surface semi-static scatterer, when the effect of this scatterer, (with anisotropy only) annuls the regional 2D-anisotropy; **(c)** for a 2D-regional structure, with the presence of a local near surface semi-static scatterer, when the effect of this scatterer, (with twist, shear and anisotropy), annuls the regional 2D-anisotropy.

The above illustrative study, through the relative MT-ESB module, clearly indicated that generally the conventional analysis, which does not perform a de-composition of the impedance tensor, fails to determine correctly the principal axes of the two-dimensional geoelectric structure.

derived. The clockwise rotation of this system's horizontal axes through an angle $\vartheta$ varying $0^o \leq \vartheta \leq 180^o$ produces a new measuring coordinate system (x′,y′), where the elements $Z'_{ij}(\vartheta)$ of the impedance tensor $\vec{Z}'(\vartheta)$ are determined from the ex-



**Fig.7** The geometrical locus of the electric field vector trace as a result of the rotation of the incident horizontal linearly polarised unitary magnetic field, **(a)** for a 2D-structure with high anisotropy; **(b)** for a 2D-regional structure with high anisotropy and the presence of a local near surface semi-static scatterer (with twist, shear and anisotropy); **(c)** same as (b) case but the co-ordinate system (of b-case) has been rotated 28° degrees counterclockwise (i.e., the strike angle determined from the conventional analysis).

# 3 MT-ESB and Mohr Circle Topology

## 3.1 Theoretical basis for MT-ESB's modules dedicated to study Mohr circles

pansion of the equation:

$$\vec{Z}'(\vartheta) = \hat{R}(\vartheta)\vec{Z}_m\hat{R}^t(\vartheta) \qquad (26)$$

where $\hat{R}$ is the rotational operator.

By taking the real parts (the procedure is identically repeated for the imaginary parts) and some trivial calculus on equation (26), Lilley [7], [8] intro-

duced Mohr circle as a tool displaying information of the magnetotelluric impedance tensor. Mohr circle is described by the relation:

$$\left(Z'_{xx_r}(\vartheta) - Z_{2_r}\right)^2 + \left(Z'_{xy_r}(\vartheta) - Z_{1_r}\right)^2 =$$

$$= \left(\frac{Z_{xy_r} + Z_{yx_r}}{2}\right)^2 + \left(\frac{Z_{xx_r} - Z_{yy_r}}{2}\right)^2 \qquad (27)$$

where the rotationally invariant quantities $Z_{1_r}$ and $Z_{2_r}$ are given respectively:

$$Z_{1_r} = \frac{Z_{xy_r} - Z_{yx_r}}{2} \quad , \quad Z_{2_r} = \frac{Z_{xx_r} + Z_{yy_r}}{2} \qquad (28)$$

and Mohr circle is depicted at a diagram of $Z'_{xx_r}(\vartheta)$ versus $Z'_{xy_r}(\vartheta)$, with the variation of the rotation angle $\vartheta$. If the point $\left(Z_{xy_r}, Z_{xx_r}\right)$ of the circle refers to the initial measuring system, the clockwise rotation of the latter at an angle $\vartheta$ produces a counterclockwise angular displacement $2\vartheta$ on the circle, i.e., to a new point $\left[Z'_{xy_r}(\vartheta), Z'_{xx_r}(\vartheta)\right]$ which refers to the new measuring system (x′,y′) [9], [10], [12].

The circle is characterized by the rotationally invariant parameters [9]:
centre coordinates: $Z'_{xy_r} = Z_{1_r}$ , $Z'_{xx_r} = Z_{2_r}$ (29)
the distance of the circle centre from the origin of the axes hereafter termed as "central impedance":

$$d = \frac{1}{2}\left[\left(Z_{xx_r} + Z_{yy_r}\right)^2 + \left(Z_{xy_r} - Z_{yx_r}\right)^2\right]^{1/2} \qquad (30)$$

radius: $R = \frac{1}{2}\left[\left(Z_{xy_r} + Z_{yx_r}\right)^2 + \left(Z_{xx_r} - Z_{yy_r}\right)^2\right]^{1/2}$ (31)

skew angle: $\gamma = \tan^{-1}\left(\frac{Z_{xx_r} + Z_{yy_r}}{Z_{xy_r} - Z_{yx_r}}\right)$ (32)

where *skew angle*, γ, is the angular deviation of the circle's centre from the $Z'_{xy_r}$-axis and is a measure of the three-dimensionality of the geoelectric structure, i.e., a structure with no specific symmetry [9].

In the case where the earth conductivity structure has an ideal 1D-symmetry, the following restrictions hold:

$$Z'_{xx}(\vartheta) = Z'_{yy}(\vartheta) = 0 \text{ and } Z'_{xy}(\vartheta) + Z'_{yx}(\vartheta) = 0$$

and it can be seen that Mohr circle degenerates to a single point, i.e., its centre which lies on the $Z'_{xy_r}$-axis.

Furthermore, in the case where the earth conductivity structure has an ideal 2D-symmetry, the following restrictions hold:

$$Z'_{xx}(\vartheta) + Z'_{yy}(\vartheta) = 0 \text{ and } Z'_{xy}(\vartheta) + Z'_{yx}(\vartheta) \neq 0$$

which at the principal axis system become:

$$Z'_{xx}(\vartheta_0) = Z'_{yy}(\vartheta_0) = 0 \text{ and } Z'_{xy}(\vartheta_0) + Z'_{yx}(\vartheta_0) \neq 0$$

and the following conclusions are drawn: (i) the centre lies on the $Z'_{xy_r}$-axis. It is evident that the departure of the centre from $Z'_{xy_r}$-axis is a measure of the deviation from two-dimensionality; (ii) the points where the Mohr circle intersects the $Z'_{xy_r}$-axis are the limits of the tensor element $Z'_{xy_r}(\vartheta)$ and the circle radius is calculated from them:

$$R = \frac{Z'_{xy_r}(\vartheta)\big|_{max} - Z'_{xy_r}(\vartheta)\big|_{min}}{2} \qquad (33)$$

In this case the radius of Mohr circle is a measure of the conductivity contrasts at the strike and dip directions, i.e., is a measure of the 2D-anisotropy; iii) the counterclockwise angular displacements $2\vartheta_0$ and $\left(2\vartheta_0 + \pi\right)$ respectively, from the circle intersections with the $Z'_{xy_r}$-axis, of the point $\left[Z'_{xy_r}(\vartheta = 0), Z'_{xx_r}(\vartheta = 0)\right]$, which refers to the measuring system, actually provide the angles $\vartheta_0$ and $\vartheta_0 + \frac{\pi}{2}$ (through which the measuring system (x,y) must be rotated clockwise in order to be aligned with the principal axes, i.e., the strike and dip directions of 2D-structure) [9], [10], [11].

Furthermore, the *"conjugate"*-form of Mohr circles (i.e. by substituting the element $Z'_{xy}(\vartheta)$ with the element $Z'_{yx}(\vartheta)$ at their construction), introduced by Makris [11], [12], yields important information concerning the regional geoelectric structure.

From the above discussion it is evident that MT-interpretation is easiest in those cases where the structure under prospection is either one-dimensional (1D) i.e., homogeneous or horizontally layered, or two-dimensional (2D) i.e., uniform along a horizontal axis (strike-direction) [6]. However, the experimentally determined MT-impedance tensor very rarely conforms to the ideal 1D or 2D-form.

By exploiting the potential of the above, briefly presented, Mohr circle theory, MT-ESB modules have been developed aiming to provide learners with powerful and in adequate extent configurable educational tools in order to thoroughly study and deeply understand the philosophy of magnetotelluric representation of Mohr circles.

## 3.2 MT-ESB 's modules dedicated to study Mohr circles

Lilley [9], [10] modified the non-linear system of complex equations (18)-(21) of the Groom and Bailey decomposition parameters t, e, σ, δ and $\vartheta$ in the new form:

$$Z_{xx} + Z_{yy} = \sigma(\tan A + \tan C) \tag{34}$$

$$Z_{xy} + Z_{yx} = \delta[(1 - \tan A \tan B)\cos 2\vartheta$$
$$- (\tan A + \tan B)\sin 2\vartheta] \tag{35}$$

$$Z_{yx} - Z_{xy} = -\sigma(1 - \tan A \cdot \tan C) \tag{36}$$

$$Z_{xx} - Z_{yy} = \delta[-(\tan A + \tan B)\cos 2\vartheta$$
$$- (1 - \tan A \cdot \tan B)\sin 2\vartheta] \tag{37}$$

by introducing the following substitutions:

$$\tan A = t \tag{38}$$

$$\tan B = \frac{e\sigma}{\delta} = \frac{\tan E}{\tan D} \tag{39}$$

$$\tan C = \frac{e\delta}{\sigma} = \tan E \cdot \tan D \tag{40}$$

$$\tan D = \frac{\delta}{\sigma} \tag{41}$$

$$\tan E = e \tag{42}$$

Consequently, the set of eqs (34)-(37) can be studied by applying Mohr circle analysis and by implementing the Mohr-modules of the developed MT-ESB. The conditional repetition of this procedure produces an *"atlas"* of different models of the geoelectric structure which belong to the general types 3D-

$$\ddot{Z}' = \ddot{T}\ddot{S}\ddot{Z}_{2D} \overset{|e|\to 1}{\approx} \begin{pmatrix} b(t\mp 1) & \alpha(1\mp t) \\ -b(1\pm t) & \alpha(t\pm 1) \end{pmatrix} \tag{43}$$

The Mohr circle parameters are:

Centre coordinates: $\left( \dfrac{\sigma \mp \delta t}{2}, \dfrac{\sigma t \pm \delta}{2} \right)$ (44)

Central impedance: $d \approx \dfrac{\delta}{2}\sec A \cdot \csc D$ (45)

Radius: $R \approx \dfrac{\delta}{2}\sec A \cdot \csc D$ (46)

Skew angle: $\gamma \approx A \pm D$ (47)

It is underscored that the equality of eqs (45) and (46) implies that the circle passes through the origin of the axes and this is verified with the associated graph produced with MT-ESB (see Fig.8).

### 3.2.2 1D-Geoelectric Structure with Strong Shear Distortion

The 1D-principal impedance tensor has the simple form:

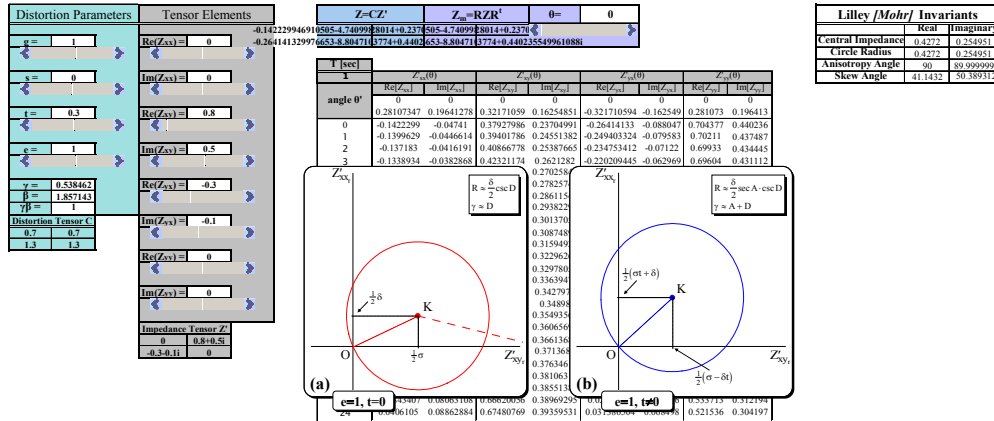$$\ddot{Z}_{1D} = \begin{pmatrix} 0 & z_0 \\ -z_0 & 0 \end{pmatrix} \tag{48}$$



**Fig.8** Mohr circles for 2D-(regional)/3D-(local) with <u>strong</u> local distortion ($|e| \to 1$): **(a)** without twist; **(b)** with twist.

(local)/2D-(regional) or 3D-(local)/1D-(regional) that can be thoroughly studied, thus enabling deep comprehension of the relevant theory.

Furthermore, as it has been shown [12], [13] this *"atlas"* can be used to resolve geoelectric structure ambiguities.

Following, two interesting geoelectric models are briefly discussed, as indicative examples of the MT-ESB application for studying Mohr circle topology.

### 3.2.1 2D-Geoelectric Structure with Strong Shear Distortion

The impedance tensor in the regional principal axis system is given by:

In this case: $\sigma = 2z_0$ and $\delta = 0$. The impedance tensor is given by:

$$\ddot{Z}' = \ddot{T}\ddot{S}\ddot{Z}_{1D} \overset{|e|\to 1}{\approx} \begin{pmatrix} z_0(t\mp 1) & z_0(1\mp t) \\ -z_0(1\pm t) & z_0(t\pm 1) \end{pmatrix} \tag{49}$$

The Mohr circle parameters are:

Centre coordinates: $\left( \dfrac{\sigma}{2}, \dfrac{t\sigma}{2} \right)$ (50)

Central impedance: $d \approx \dfrac{\sigma}{2}\sec A$ (51)

Radius: $R \approx \dfrac{\sigma}{2}\sec A$ (52)

Skew angle: $\gamma = A$ (53)

We remind that in ideal 1D-geoelectric structure the Mohr circle degenerates to its centre. Therefore, the presence of 3D-distortion moves the centre away

from the $Z'_{xy_r}$-axis and takes place a "circular dilation" of the point-circle at the new position. This is illustrated very well by the relevant MT-ESB module (see Fig.9). The equality of eqs (51) and (52) implies once more that the Mohr circle passes through the origin of the axes and again this is verified with the associated graph from MT-ESB (see Fig.9).
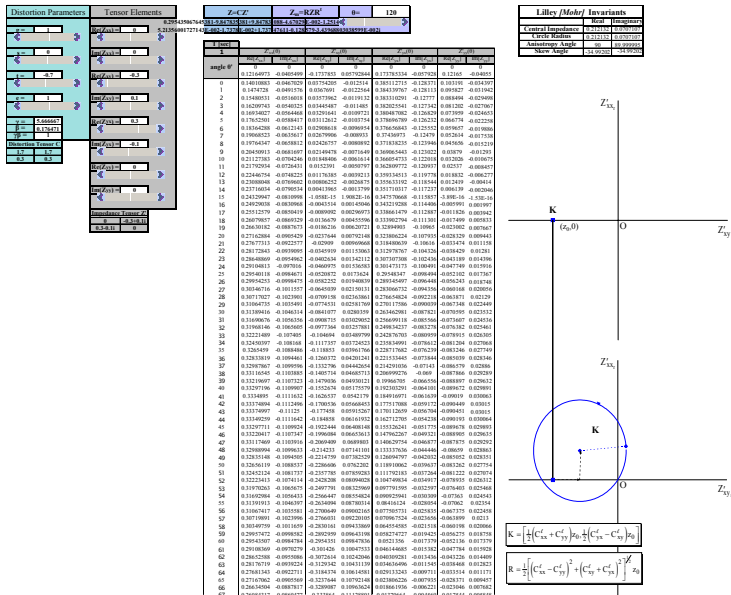


**Fig.9** Mohr circles: (i) *upper diagram:* for 1D-geoelectric structure (the circle degenerates to its centre), (ii) *lower diagram:* for 1D-(regional)/3D-(local) with <u>strong</u> local distortion ($|e| \rightarrow 1$).

## 4 Conclusions

Aiming to offer an educational tool that will diminish the difficulties reported in teaching magnetotellurics from both sides, i.e., learners and tutors, a Magnetotelluric Educational Software Bundle, (MT-ESB) was developed.

The configurable modules of MT-ESB concerning the study of impedance tensor decomposition, distortion tensor decomposition, and Mohr circle topology were presented through indicative examples of specific geoelectric structures with predefined theoretical symmetries.

## 5 Acknowledgements

*References:*

[1] K. Bahr, *Magnetotellurische Messung des Elektrischen Widerstandes der Erdkruste und des Oberen Mantels in Gebieten mit Localen und Regionalen Leitfahigkeitsanomalien*, Doctoral thesis, Gottingen, 1985.

[2] M.N. Berdichevsky, V.I. Dmitriev, Basic principles of interpretation of magnetotelluric curves, in Geoelectric and Geothermal Studies, A.Adam, Ed., *Akademini Kiado*, 1976, pp. 165-221.

[3] R.W. Groom, *The Effects of Inhomogeneities on Magnetotellurics*, Ph.D. Thesis, University of Toronto, Canada, 1988.

[4] R.W. Groom and R.C. Bailey, Decomposition of magnetotelluric impedance tensors in the presence of local three-dimensional galvanic distortion, *J. Geophys. Res.,* vol 94, 1989, pp. 1913-1925.

[5] R.W. Groom, D.R. Kurtz, G.A. Jones, E.D. Boemer, A quantitative methodology to extract regional magnetotelluric impedances and determine the dimension of the conductivity structure, *Geophys. J. Int.,* vol 115, 1993, pp. 1095-1118.

[6] A.A. Kaufman and G.V. Keller, The Magnetotelluric Sounding Method, *Elsevier*, Amsterdam, 1981.

[7] T. Lilley, Diagrams for magnetotelluric data, *Geophysics*, Vol.41, 1976, pp. 766-770.

[8] T. Lilley, J.H. Filloux, I.J. Ferguson, N.L. Bindoff, and P.J. Mulhearn, The Tasman project of seafloor magnetotelluric exploration: Experiment and observations, *Phys. Earth Planet. Int.*, Vol.53, 1989, pp. 405-421.

[9] T. Lilley, Magnetotelluric analysis using Mohr circles, *Geophysics*, Vol.58, 1993, pp. 1498-1506.

[10] T. Lilley, Mohr Circles in Magnetotelluric Interpretation (i) Simple static Shift (ii) Bahr's Analysis, *J. Geomag. Geoelectr.*, Vol.45, 1993, pp. 833-839.

[11] J.P. Makris, *Electromagnetic study of the geoelectric structure of an area sensitive to the detection of pre-seismic electric signals*, Ph.D. Thesis, Dept. of Physics, University of Athens, Greece, 1997.

[12] J. Makris, N. Bogris, and K. Eftaxias, A new approach in the determination of characteristic directions of the geoelectric structure using Mohr circles, *Earth Planets Space*, Vol.51, 1999, pp. 1059-1065.

[13] J.P. Makris, F.K. Vallianatos and I.O. Vardiambasis, "Tensor Decomposition Resolves Geoelectrical Structure Modeling Ambiguities in Mohr Circle Topology", *in Special Issue on "Optimization, Simulation, Modeling and Control in Systems Sciences", WSEAS Transactions on Circuits and Systems, 2,* Issue 3, July 2003, pp. 561-568.

[14] W.E. Sims, F.X. Bostick Jr., *Methods of magnetotelluric analysis*, Res. Lab. tech. rep. no. 58, Univ. of Texas, Austin, 1969.

[15] S. Spitz, The Magnetotelluric impedance tensor properties with respect to rotations, *Geophysics*, vol 50, No 10, 1985, pp. 1610-1617.

[16] M.C. Swift Jr., *A magnetotelluric investigation of an electrical conductivity anomaly in the southwestern United States*, Ph.D. thesis, Mass. Inst. of Tech., MA, 1967.

[17] J. Walkenbach, *Excel 2003 Bible*, Wiley Publishing, Inc., 2003.

[18] P. Zhang, R.G. Roberts, L.B. Pedersen, Magnetotelluric strike rules, *Geophysics*, vol 51, 1987, pp. 267-278.